Time-dependent Study Of Pressure Waves Generated By Square Array MEMS Ultrasound Transducers

M.A.G. Suijlen[1], R. Woltjer[1]
1. Novioscan BV, Nijmegen, The Netherlands

Introduction

For non-imaging echo sounding applications in the human body Novioscan is developing piezoelectric micromachined ultrasound transducers (PMUT). Here, transducers send intermittent ultrasonic pulses into the body and detect their echoes to measure for example bladder size [1].

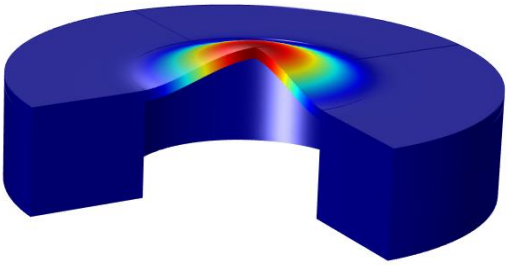

Figure 1. Single circular membrane of PMUT with deflected surface when excited.

The developed PMUTs contain a large number of micromechanical silicon membranes with piezoelectrically actuated regions to generate ultrasonic pressure waves in the patient's body.

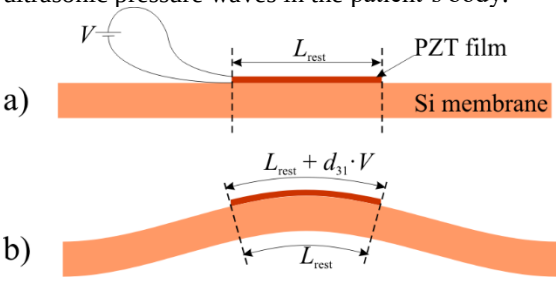

Figure 2. Actuation of membrane by local expansion / contraction of piezoelectric material (PZT) film. An electrostatic voltage across the film thickness, a), translates via in-plane expansion to an out-of-plane displacement, b).

For Novioscan's bladder monitor, circular membranes of resonant frequency in the low MHz range are a suitable starting point for designing and modeling a prototype PMUT.
Actuation of the circularly clamped membranes happens through the local expansion and contraction of a piezoelectric material film on top of the silicon surface (**Figure 2**).
Figure 3 shows a cross section of the simulated SOI-based piezoelectric MEMS circular diaphragm. The top electrode covers 56% of the size of the diaphragm, roughly the area that has a positive curvature, where the rest has a negative one, or vice versa. This ensures a most efficient ultrasound generation.

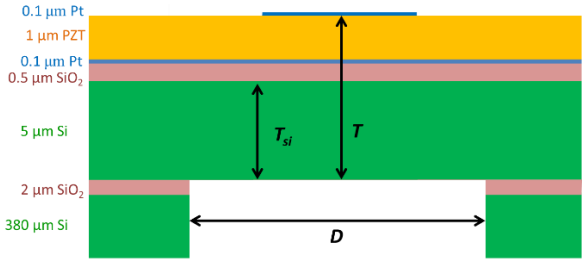

Figure 3. Cross section view of circular membrane used in this article. Membrane diameter *D* equals 100 µm.

Analytic model

For a membrane consisting of a stack of *N* layers, where each layer, numbered *i*, has thickness T_i, we can calculate the moment M_{piezo} due to the piezoelectric actuation of the PZT layer by a voltage *V* [1]:

$$M_{\text{piezo}} = \frac{d_{31,f} \cdot Y_{\text{PZT}}}{(1-\nu_{\text{PZT}}^2)} \frac{V}{T_{\text{PZT}}} \int_{t_i}^{t_i+T_{\text{PZT}}} (t - t_n) \mathrm{d}\, t$$

with

- $d_{31,f}$, transverse piezoelectric coefficient for a PZT layer fixed on a rigid substrate,
- Y_{PZT}, Young's modulus of the PZT layer material,
- t_i, coordinate of the bottom of the PZT layer,
- ν_{PZT}, Poisson ratio for PZT.

[1] **"De activiteiten worden mede mogelijk gemaakt door de Europese Unie en het Europees Fonds voor Regionale Ontwikkeling."**

We estimate the moment due to the piezoelectric actuation for a diaphragm of total thickness T, consisting of mainly a silicon layer of thickness T_{si}, topped by a stack *N-1* thin layers of thickness T_i with material properties with index i, where the PZT layer is on top:

$$M_{\text{piezo}} \approx \frac{d_{31,f}\, Y_{\text{PZT}}\, V}{2\,(1-\nu_{\text{PZT}}^2)}\left(2T - T_{\text{si}} - T_{\text{PZT}} - \frac{T\cdot T_{\text{corr},Y}}{T_{\text{Si}}+T_{\text{corr},Y}}\right)$$

with

$$T_{\text{corr},Y} = \frac{Y_{\text{PZT}}}{Y_{\text{Si}}}\,T_{\text{PZT}} + \frac{Y_{\text{Pt}}}{Y_{\text{Si}}}\,T_{\text{Pt}} + \frac{Y_{\text{SiO2}}}{Y_{\text{Si}}}\,T_{\text{SiO2}}$$

Table 1. Material properties of layers in used membrane (**Figure 3**).

Material	T_i (µm)	d_{31} (pm/V)	ρ_i (kg/m³)	Y_i (GPa)	ν_i	ρ_i/ρ_{Si}	$T_{corr,\rho}$	Y_i/Y_{si}	$T_{corr,Y}$
Pt	0.0		21090	138	0.25	9.1	0.0	0.9	0.0
PZT	1.0	123	7500	95.2	0.35	3.2	3.2	0.6	0.6
Pt	0.1		21090	138	0.25	9.1	0.9	0.9	0.1
SiO_2	0.5		2200	70	0.17	0.9	0.5	0.4	0.2
Si	5.0		2329	169	0.064	1.0		1.0	
Membrane	6.6						4.6		0.9

Static deflection for a circular clamped diaphragm, consisting of mainly a silicon layer of thickness T_{Si} and *N-1* thin top layers of thickness T_i of material i, with PZT layer close to the top, is found to be [1]:

$$z_{0,\,\max} = \int_0^{\frac{1}{2}D_{\text{eff}}} \frac{1}{s}\int_0^{R_{in}} \frac{M_{\text{piezo}}}{D_m}\, r\ \mathrm{d}r\,\mathrm{d}s$$

$$\approx 3\, d_{31,f}\,\frac{(1-\nu_{Si}{}^2)}{(1-\nu_{\text{PZT}}{}^2)}\,\frac{Y_{\text{PZT}}}{Y_{Si}}\,V\,\frac{{R_{in}}^2}{{T_{Si}}^2}\ln\left(\frac{D_{\text{eff}}}{2\,R_{in}}\right)\cdot\zeta$$

with

- $D_{\text{eff}} = D + 1.5\,T$, with membrane diameter D and total membrane thickness T,
- $z_{0,\max}$, maximum static displacement at the membrane centre,
- R_{in}, inner diameter of the top electrode,
- $D_m \approx \frac{Y_{Si}\,{T_{Si}}^2}{12(1-\nu^2)}\left[T_{Si} + 3T_{\text{corr},Y}\left(1 + 2\frac{T-T_{Si}}{T_{Si}} - \frac{T_{\text{corr},Y}}{T_{Si}}\right)\right]$,
- $\zeta \equiv \frac{2T-T_{Si}-T_{\text{PZT}}-\frac{T\cdot T_{\text{corr},Y}}{T_{Si}+T_{\text{corr},Y}}}{T_{Si}+3\frac{T_{Si}\,T_{\text{corr},Y}}{(T_{Si}+T_{\text{corr},Y})}\left(\frac{T}{T_{Si}}\right)^2}$

Considering the deflection of the membrane as a function of radial coordinate r:

$$z(r) = z_{0,\,\max}\cdot\left(1-\left(\frac{2r}{D_{\text{eff}}}\right)^2\right)^2,$$

the surface averaged displacement $z_{0,\text{avg}}$ turns out to be one third of the maximum static displacement:

$$\mathrm{z}_{0,\,\text{avg}} = \frac{8}{{D_{\text{eff}}}^2}\int_0^{\frac{1}{2}D_{\text{eff}}} z(r)\ r\,\mathrm{d}r = \frac{1}{3}\mathrm{z}_{0,\,\max}$$

Newton's law of force yields a differential equation for the time dependence of the average displacement z_{avg} of the circular membrane with damping coefficient $b_{\text{m,plate}}$ and driven by an oscillatory force F_{piezo} with an acoustic medium on one side that influences the membrane by the force F_{aco}.

$$m_{\text{plate}}\ddot{z}_{\text{avg}} + b_{\text{m,plate}}\dot{z}_{\text{avg}} + k_{\text{plate}}z_{\text{avg}} = F_{\text{piezo}} - F_{\text{aco}}$$

$$\Rightarrow\ m_{\text{plate}}\ddot{z}_{\text{avg}} + \left(b_{\text{m,plate}} + Z_{\text{rad}}\right)\dot{z}_{\text{avg}} + k_{\text{plate}}z_{\text{avg}} = F_{\text{piezo}}$$

with

- m_{plate}, effective mass of the membrane,
- k_{plate}, stiffness of the membrane,
- $b_{\text{m,plate}}$, mechanical damping coefficient of the membrane,
- F_{piezo}, total force by the PZT material on the membrane,
- F_{aco}, total force on the membrane by the acoustic medium on one side of the membrane,
- Z_{rad}, complex-valued radiation impedance.

The radiation impedance Z_{rad} describes the interaction of a transducer with the acoustic medium, thus we take $F_{\text{aco}} \approx Z_{\text{rad}}\,\dot{z}_{\text{avg}}$, where $\dot{z}_{\text{avg}}$ is the velocity of the membrane, averaged over its surface area. The complex radiation impedance is conventionally split into $Z_{\text{rad}} = R_{\text{rad}} + j\,X_{\text{rad}}$.

The real part, R_{rad}, called the radiation resistance, denotes the amount of the power radiated to the medium; whereas the imaginary part, X_{rad}, the radiation reactance, shows the stored energy in the near field. At lower frequencies, the real part and the imaginary part of the radiation impedance can be approximated as [2]:

$$Re(Z_{\text{rad}}) = R_{\text{rad}}(\omega) \approx \frac{1}{2}\rho_{\text{aco}}\,c_{\text{aco}}\,A\left(\frac{\omega D_{\text{eff}}}{2c_{\text{aco}}}\right)^2$$

$$= \frac{\pi\,\rho_{\text{aco}}}{32\,c_{\text{aco}}}{D_{\text{eff}}}^4\omega^2$$

with

- ρ_{aco}, mass density of the acoustic medium,
- c_{aco}, sound velocity in the acoustic medium,
- A, surface area of the membrane.

$$Im(Z_{rad}) = X_{rad}(\omega) \approx 2h_{00}\,\rho_{aco}\,c_{aco}\,A\left(\frac{\omega D_{eff}}{2c_{aco}}\right) = h_{00}\,\rho_{aco}\,\frac{\pi}{4}D_{eff}^3\,\omega \equiv m_{aco}\,\omega$$

with

- m_{aco}, effective mass loading of the acoustic medium on the membrane,
- h_{00} = 0.335, effective thickness of the acoustic medium load on the membrane as a fraction of D_{eff} [3].

This result allows us to write the membrane's equation of motion as follows:

$$(m_{plate} + m_{aco})\ddot{z}_{avg} + (b_{m,plate} + R_{rad})\dot{z}_{avg} + k_{plate}z_{avg} = F_{piezo}$$

Setting initial conditions to $z_{avg}(0)=0$ and $\dot{z}_{avg}(0) = 0$ the transient solution for $z_{avg}(t)$ can be found from the convolution integral [4]:

$$z_{avg}(t) = \frac{\int_0^t F_{piezo}(t-h)e^{-\gamma h}\sin\omega_1 h \cdot dh}{(m_{plate}+m_{aco})\omega_1}$$

with

- $\gamma = \frac{b_{m,plate}+R_{rad}}{2(m_{plate}+m_{aco})}$,
- $m_{plate} = \frac{48\,\pi}{10.22^2}\rho_{si}(T_{si} + T_{corr,\rho})D_{eff}^2$,
- $k_{plate} = 768\pi\,\frac{D_m}{D_{eff}^2}$,
- $\omega_1 = \sqrt{\frac{k_{plate}}{(m_{plate}+m_{aco})} - \gamma^2}$,

and

$$F_{piezo} = 128\pi\,M_{piezo}\frac{R_{in}^{\ 2}}{D_{eff}^{\ 2}}\ln\left(\frac{D_{eff}}{2\,R_{in}}\right)$$

Table 2. Parameter values for the membrane in current study.

Parameter	Value	Unit
D	100	µm
T	6.6	µm
D_{eff}	109.9	µm
R_{in}	25.0	µm
D_m	3.15	10^{-6} Nm
$\partial M_{piezo}/\partial V$	41.3	10^{-6} N/V
ζ	0.674	
$\partial z_{0,max}/\partial V$	3.01	10^{-9} m/V
k_{plate}	0.628	10^{6} N/m
m_{plate}	0.391	10^{-9} kg

For the pressure amplitude generated in the far-field p_{ff}, we approximate the MEMS membrane by a piston of the same area and we take the displacement averaged over this area:

$$p_{ff}(s) = p_0\frac{R_0}{s} = \rho_{aco}c_{aco}u_{avg}\frac{A}{\lambda s} = \frac{\rho_{aco}}{8}\frac{\omega}{s}D_{eff}^2\,u_{avg}$$

- s, perpendicular distance to the MEMS membrane,
- $p_0=\rho_{aco}\,c_{aco}\,u_{avg}$, theoretical surface pressure,
- ρ_{aco}, density of acoustic medium,
- c_{aco}, sound velocity in acoustic medium,
- u_{avg}, velocity of the membrane averaged over the effective surface area.
- $R_0=A/\lambda$, Rayleigh distance,
- A, surface area of the membrane,
- λ, wavelength of pressure wave.

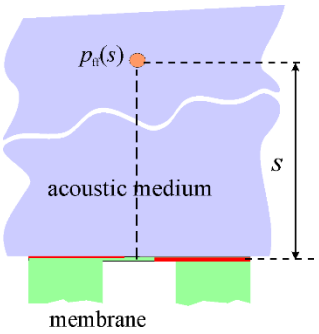

Figure 4. Far-field acoustic pressure p_{ff} at a distance s of the membrane transducer.

Simulation model

The simulation model describes the development in time of membrane amplitude and transmitted acoustic pressure in water upon excitation by a voltage pulse on the piezoelectric layer of the membrane. Beginning with an isolated, single membrane, simulations were run on simultaneously excited membranes in 2x2, 3x3 and 4x4 square arrays (**Figure 5**).

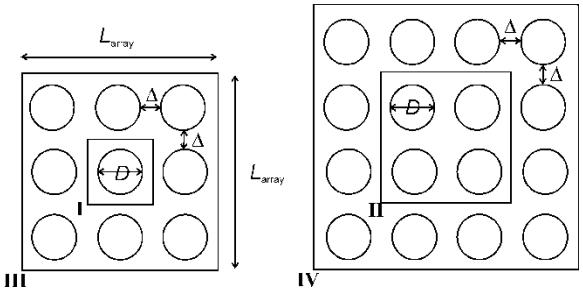

Figure 5. Simulated PMUTs as single (I) membrane, 2x2 (II), 3x3 (III) and 4x4 (IV) square arrays of these membranes.

COMSOL 5.2 with Acoustics Module was used to build a 3D model from the pre-defined **Acoustic-Piezoelectric Interaction, Transient** interface. Via nodes in the added branches for **Solid Mechanics**, **Electrostatics** and **Pressure Acoustics** physics interactions are controlled in detail.

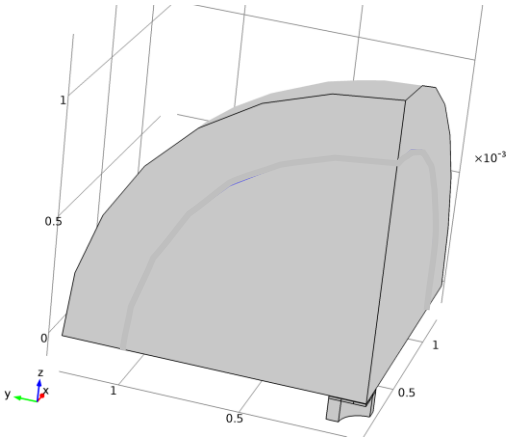

Figure 6. Geometry of COMSOL simulation model. The quarter hemispherical part represents the acoustic water domain.

A geometry for the simulation model must represent the application of an ultrasound transducer transmitting sound into an unbounded space of the acoustic medium (**Figure 4**). Given the planar symmetry of the respective structures in both yz- and zx-plane, we create a 3D model geometry as shown in **Figure 6**. Thus, only mesh distributions on domain parts constituting one quarter of the true configuration are needed, which alleviates the computational effort accordingly.
The acoustic water domain is shaped as a hemisphere with a radius of $5L_{\text{array}}$ to absorb waves transmitted from the transducer equally in all directions. A radiation boundary condition on the outer surface allows the outgoing waves to leave the modeling domain with minimal reflections, simulating the unbounded expanse of the water domain.
The transducer models are attached to the hemisphere center and take into account the planar symmetries: the circular membrane transforms into a quarter pie (**Figure 7**). Materials are assigned according to the cross section view in **Figure 3** and have properties according to **Table 1**.

Pulse excitation and solver settings

The membrane is excited by a Gaussian voltage pulse on the top electrode (**Figure 7**), defined as:

$$V(t) = V_0 \cdot e^{-2\pi^2 (f_{\text{pulse}} t - 1)^2}$$

As can be shown from the Fourier transform of this function, the frequency spectrum of the pulse cuts off sharply at f_{pulse}. As a result, the generated pressure variations in the acoustic domain will not have wavelengths shorter than $c_{\text{aco}}/f_{\text{pulse}}$, limiting the required mesh resolution.
In the solver settings, time-step size is fixed using a CFL number of 0.05 to limit temporal discretization errors in the generalized-α solving method [5].

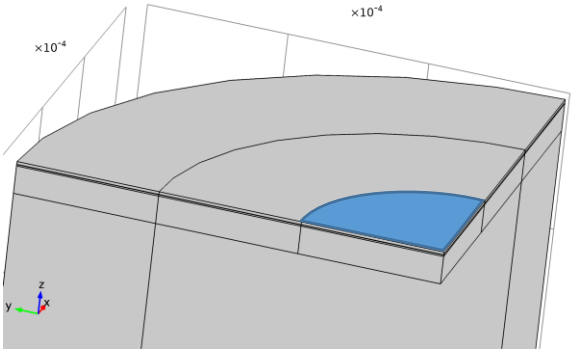

Figure 7. Transducer membrane and electrode area (shaded).

Mesh

Structured mesh distributions are generated in the domains of the transducer to achieve best element quality with the least amount of elements.
In the acoustic medium domain, we generate a free tetrahedral mesh to ensure isotropic solution conditions for radiated pressure waves.

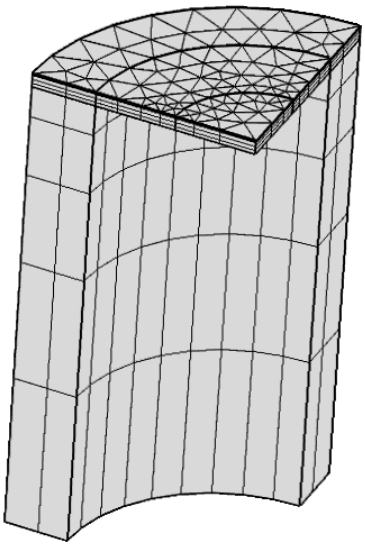

Figure 8. Structured mesh distribution used for every membrane in the array.

Here, the maximum mesh size, yielding a proper sampling of radiated pressure waves, is set to 1/6th of the smallest wavelength generated during the pulse excitation. This wavelength is the speed of sound in water (1481 m/s) divided by the cut-off frequency, f_{pulse}, of the voltage pulse frequency spectrum. All other tetrahedral mesh parameters are kept relaxed. The structured mesh of the transducer begins with a triangular boundary mesh on the top surface which is extruded through the layers in the membrane part. A second extrusion is performed for the thicker handle layer part.

Table 3. Parameter values used in simulations of pulse excited square membrane arrays of 1x1, 2x2, 3x3 and 4x4 sizes.

Parameter	Value	Unit
D	100	µm
Δ	50	µm
f_{pulse}	4.0	MHz
V_0	1.0	V
m_{aco}	0.349	10^{-9} kg
R_{rad}	6.13	10^{-3} kg/s
$b_{\text{m,plate}}$	0.00	10^{-3} kg/s
γ	4.13	10^{6} rad/s
ω_1	28.8	10^{6} rad/s
ρ_{water}	998	kg/m^3
c_{water}	1481	m/s

Simulation Results and Discussion

For square membrane arrays of 1x1, 2x2, 3x3 and 4x4 size with parameter values according to **Table 3**, the simulations result in a rich collection of data on membrane displacement and pressure variations in the water domain.

The time development of the membrane center displacement shows well how the water dampens the membrane motion (**Figure 9**). The generated pressure wave as a result of this displacement then travels along the acoustic axis in about 1.5 µs to the edge of the water domain (**Figure 10**).

As shown in **Figure 11** the peak pressure of the wave has decayed considerably on this edge. Using a 1/s fit model on the furthest points of the decay curve (s > 1.2 mm), we extrapolate the acoustic peak pressure in the far-field for each array.

This results in the graph of **Figure 12** where we see that the generated pressure of the array is entirely proportional to the number of membranes. A linear fit forced through the origin indicates a pressure level of 10.9 Pa per membrane at 100 mm distance. If we compare this to the analytic result from

$$p_{\text{ff}}(s) = \frac{\pi}{4}\frac{f_{\text{pulse}}}{s}\rho_{\text{water}}D_{\text{eff}}^2\,u_{\text{peak, avg}}$$

with

$u_{\text{peak, avg}} = 0.030\ {}^{\text{m}}/_{\text{s}}$, computed from the time-derivative of

$$z_{\text{avg}}(t) = \frac{\int_0^t F_{\text{piezo}}(t-h)e^{-\gamma h}\sin\omega_1 h\cdot \mathrm{d}h}{(m_{\text{plate}}+m_{\text{aco}})\omega_1}$$

reading

$$p_{\text{ff}}(0.1\text{ m}) = 11.4\text{ Pa}$$

we find a great agreement of simulation with theory.

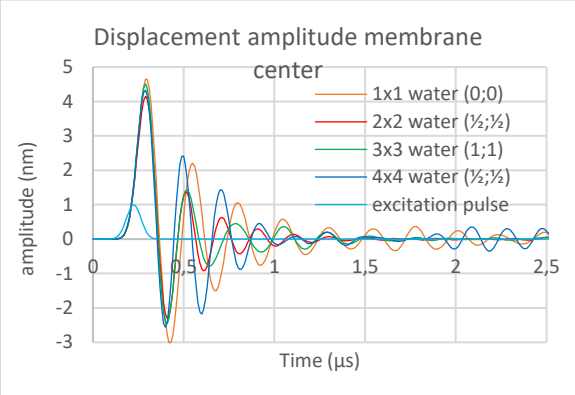

Figure 9. Time development of membrane center displacement in water as a result of the 1 Volt excitation pulse.

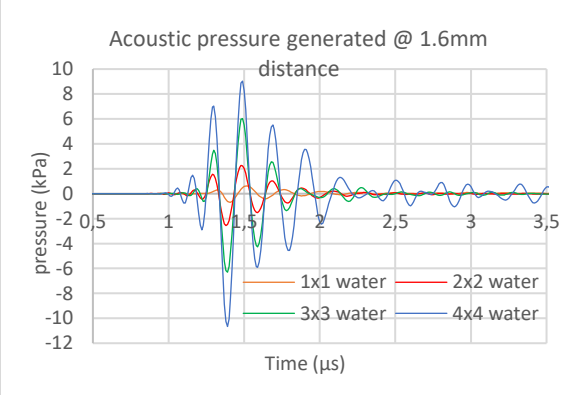

Figure 10. Time development of acoustic pressure in water at 1.6 mm distance from the membrane array surface as a result of the 1 Volt excitation pulse.

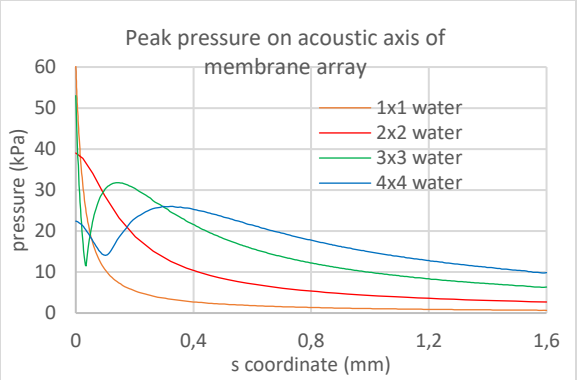

Figure 11. Decay of peak pressure values in the generated pulse train of **Figure 10** along the acoustic axis of the membrane arrays.

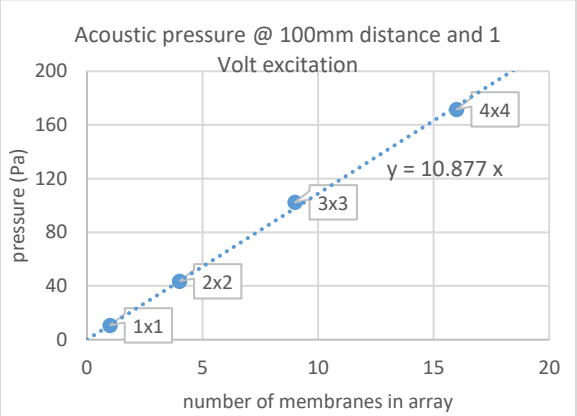

Figure 12. Dependency of far-field acoustic pressure at 100 mm distance on number of membranes in the array.

In a parametric study, we simulated acoustic pressures and derived far-field peak pressure values by the 4x4 membrane array as a function of pulse duration (**Figure 13**). Although peak pressure at 100 mm decreases steadily with pulse duration, defined as $1/f_{pulse}$, the acoustic impedance Z_{aco} (i.e. pressure/ volume velocity) shows a maximum at a duration of 0.25 µs or f_{pulse} = 4.0 MHz. This is logical given the resonance frequency of the membranes in water, $f_1 = \omega_1/(2\pi)$ = 4.6 MHz.

As a last result, we present the dependency of far-field acoustic pressure at 100 mm on distance between membranes, Δ (**Figure 14**). Interestingly, acoustic pressure appears to be minimum for an intermembrane distance Δ equal to the membrane diameter D of 100 µm.

Conclusions

We present a series COMSOL simulations in full 3D piezo-acoustics for the time-dependent study of pressure waves generated by square array piezoelectric MEMS ultrasound transducers (PMUT). Finding good agreement of the simulation results with theory, we establish a reliable method for the simulation based design of new PMUTs in pulsed operation mode.

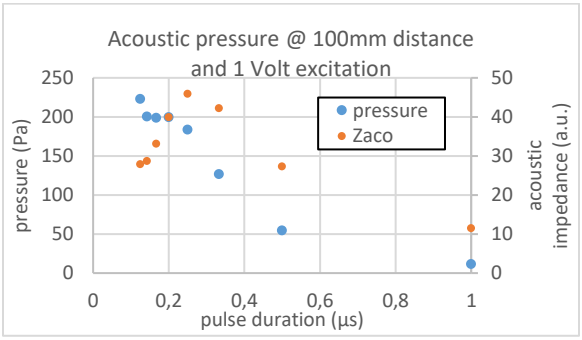

Figure 13. Dependency of far-field acoustic pressure at 100 mm distance generated by a 4×4 membrane array on duration of the 1 Volt excitation pulse.

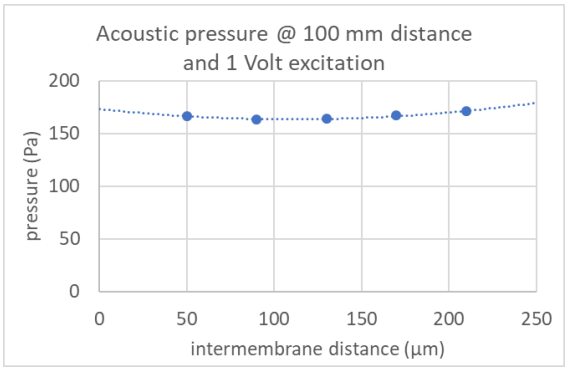

Figure 14. Dependency of far-field acoustic pressure at 100 mm distance generated by a 4×4 membrane array on distance between membranes Δ.

References

1. R. Woltjer, M. Suijlen, P. Srinivasa, N. Banerjee, J.J. Koning, A.J.H.M. Rijnders, "Optimization of piezo-MEMS layout for a bladder monitor," *IEEE Intl. Ultrasonics Symp. Proc.*, 2016.
2. L.E. Kinsler et al., *Fundamentals of acoustics*, p. 186. John Wiley & Sons, New York (2000)
3. Horace Lamb, *On the Vibrations of an Elastic Plate in Contact with Water*, Proceedings of the Royal Society of London, volume 98, issue 690, 1920, pp. 205-216.
4. G. B. Arfken et al, *Mathematical methods for physicists*, p. 906. Academic Press (1995).
5. COMSOL 5.2, *Transient Gaussian Explosion*, p. 265. Acoustics Module Application Library Manual (2015).